Acta Medica
Okayama

Original Article

In Vitro Evaluation of a Newly Developed Implantable Artificial Lung

Hitoshi Sato[a], Ichiro Taga[b], Takahiro Kinoshita[a], Akio Funakubo[c], Shingo Ichiba[d]*, and Nobuyoshi Shimizu[a]

[a]*Department of Cancer and Thoracic Surgery, Okayama University Graduate School of Medicine, Dentistry and Pharmaceutical Sciences, Okayama 700-8558, Japan,* [b]*Kawasumi Laboratories INC., Tokyo 140-8555, Japan,* [c]*Department of Electronics and Computer Engineering, Tokyo Denki University, Saitama 350-0394, Japan, and* [d]*Department of Emergency Medicine, Okayama University Hospital, Okayama 700-8558, Japan*

A prototype of an implantable artificial lung without a pump (Prototype II) has been tested. A commercially available membrane oxygenator, MENOX AL6000α® (Dainippon Ink and Chemicals, Inc., Tokyo, Japan), was used as a basic model. The packing density of the hollow fiber was decreased in order to achieve low resistance through the blood pathway. The configuration of its housing was also re-designed using computational fluid dynamics (CFD). The first prototype, known as Prototype I, was already tested in a 15 kg pig, which showed excellent gas exchange with normal hemodynamics. A second prototype, Prototype II, has a larger membrane surface area than Prototype I. The device was evaluated for resistance through the blood path and gas transfer rate in an *in vitro* setting by the single pass method using fresh bovine blood. The resistance through the blood path of Prototype II was 2.7 ± 0.7 mmHg/(L/min) at $\dot{Q}$ = 5L/min. The oxygen (O_2) transfer rate was 178 ± 5.3 ml/min at $\dot{Q}$ = 5 L/min, V/Q = 3, and the carbon dioxide (CO_2) transfer rate was 149 ± 28 ml/min at $\dot{Q}$ = 5 L/min, V/Q = 2 ($\dot{Q}$: blood flow rate, $\dot{V}$: sweep oxygen flow rate through the artificial lung). For the purpose of implantation, this prototype showed sufficiently low resistance in the pulmonary circulation with reasonable gas exchange.

Key words: artificial lung, low resistance, gas exchange, computer fluid dynamics

An implantable, low-resistance artificial lung that can be attached in the pulmonary circulation without a pump has been developed and its gas exchange capacity has been evaluated in an *in vitro* setting. In the last decade, lung transplantation has been established to treat severe respiratory insufficiency. However, a lack of appropriate donors is a serious problem with this approach. According to the Organ Procurement and Transplantation Network / Scientific Registry of Transplant Recipients 2004 annual report (<http://www.optn.org/AR2004/default.htm> 8/7/2005), over 75% of patients waited for more than 11 months for a transplant. An implantable artificial lung could play an important role as a bridge to lung transplantation in such patients. The conventional way of supporting these patients has some limitations that inhibit its long-term use. A mechanical ventilator may injure the native lung and cannot maintain gas exchange over a long term. Extracorporeal membrane oxygenation

(ECMO) can support these patients waiting for donor organs for up to 1 or 2 months, because it requires blood transfusions due to hemolysis caused by the pump.   Moreover, neither a mechanical ventilator nor ECMO is ambulatory. A pumpless artificial lung is more suitable for long-term use. In the pulmonary circulation, the biggest concerns related to the long-term use of an implantable artificial lung are right ventricular failure and the deterioration of gas exchange. Currently, resistance through the blood path is the focus of attention in the continuing development of the device.

The concept of CFD helps in judging the function of the artificial lung, predicting the location of low-blood-flow-velocity region that could generate blood clots [1], predicting a membrane oxygenator pressure drop [2], and designing the configuration of the artificial lung. The geometry of Prototype II was determined using the CFD concept. By modifying a commercially available device, we maintain a low cost of development. Menox AL 4000 α [®] and AL 6000 α [®] are both commercially available oxygenators used for cardiopulmonary support in Japan. These oxygenators have much higher blood path resistance than the native pulmonary circulation, because they are supported by a blood pump. The packing density of the hollow fibers was reduced from an original level of 40% to 25% in order to decrease the resistance through the blood path. The geometry of the housing was re-designed for use in intra-thoracic implantation according to the concept of CFD. Prototype I was already tested in the pulmonary circulation from the pulmonary artery to the left atrium using a 15 kg pig model, and it demonstrated reasonable gas exchange and hemodynamics for at least 6 h [3]. However, Prototype I was developed using Menox AL 4000 α [®] as the original model. Menox AL 4000 α [®] was originally designed for child and neonate use, and the membrane surface area is small for large animals. Prototype II was developed using a bigger model and was intended for implantation in larger animals. In this study, basic data including the pressure drop and gas exchange capacity of Prototype II were measured in an *in vitro* setting.

Materials and Methods

A DIC fiber mat (Dainippon Ink and Chemicals,

Inc., Tokyo, Japan) was packed in the polyurethane box-shaped rigid housing. The DIC fiber was made with poly methyl pentine, and it had a dense thin skin layer on the outer surface of the membrane hollow fibers, which prevented plasma leakage. The inner diameter was 165 μm and the outer diameter was 225 μm. These fibers were packed in a rigid box with the dimensions $30 \times 66 \times 95$ mm. The inner diameter of each of these inlet and outlet sockets was 12.5 mm. The inlet and outlet ports of the prototype were located side by side on the housing box in an easily accessible location so that it was easy to attach them to the pulmonary artery and the left atrium. Blood flow characteristics, namely pressure drop and flow velocity, were analyzed using CFD software (STAR LT, CD Adapco, Yokohama, Japan). The height of the housing dome (h) and the length of the taper (t) varied in these models (Fig. 1). Given that each model could have an h value representing the height of dome of h 12, 15, or 18, and that each could have a t value representing the taper length of t0, 20, 40, 48, 60, or 80, a total of 19 models were constructed involving the various permutations of these values. All 19 models had the same membrane surface area (0.72 m²) and the same priming volume (247 ml). The pressure drop through the Prototype II and the flow velocity were calculated by solving the equation of continuity (1) and the Navier-Stokes equation (2) governing fluid flow through the model. STAR-LT utilizes the finite volume method to solve these govern-
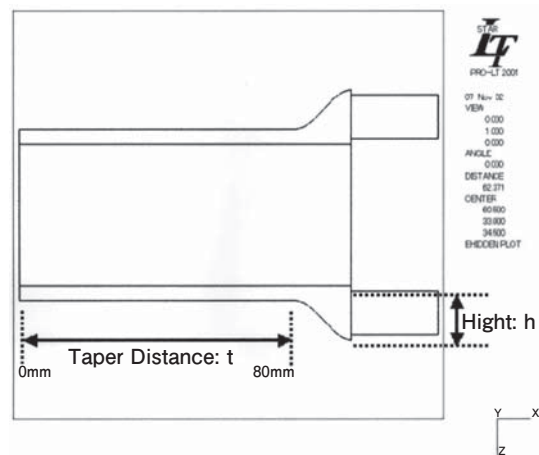

Fig. 1   Housing design with CFD: "t" indicated the taper distance, and "h" indicated the height of inlet and outlet. 19 combination of each (h, t) models were considered and the best model was selected using a CFD simulation.

ing equations:

$$\rho\left[\frac{\partial V}{\partial t} + (V \cdot \nabla)V\right] = -\nabla p + \mu\nabla^2 V \qquad (1)$$

$$div V = 0 \qquad (2)$$

where ρ was the fluid density, V was the flow velocity, p was the static pressure and μ was the dynamic fluid viscosity.

The model was designed with dimensions of $30\times 66\times 95$ mm. The model was divided into 571,968 elements. The volume of each element was 1 mm³. The boundary conditions applied in the numerical simulation were based on the conditions encountered during the water experiments. A velocity boundary condition was specified at the domain inlet. Steady laminar flow was assumed in all cases. The fluid was assumed to be incompressible ($\rho = 1060$ kg/m³) and possess a Newtonian viscosity ($\mu = 3.3$ cP) consistent with that of blood at 37℃. A constant pressure boundary condition was set for the domain outflow. The no-slip condition was enforced at the wall boundaries, and a symmetry condition was applied along the appropriate plane. Direct numerical simulation of the flow around the individual fibers of the present fiber bundle was impossible using today's technology [4]. To overcome this limitation, a porous media model that accounted for the tortuosity of the fiber bundle was used. Momentum losses were approximated using Darcy's Law:

$$\frac{\partial p}{\partial \xi_i} = -K_i u_i = -(\alpha u_i + \beta u_i)$$

where p was the static pressure, α and β represented the fiber bed permeability and u the superficial velocity (volumetric flow rate divided by fiber bundle frontal surface area). The losses predicted by the porous media model were incorporated into the momentum balance equation using Ergus's law:

$$\frac{P_0 - P_z}{Z} = \frac{1.75\rho(1-\varepsilon)}{\varepsilon^3 D_p}u^2 + \frac{150\mu(1-\varepsilon)^2}{\varepsilon^3 D_p^2}u$$

where ρ was the fluid density, P_0 and P_z were the pressure at the inlet and outlet, Z was the blood path length, μ the dynamic fluid viscosity, ε was the porository of porous media, and D_p was the outer diameter of each hollow fiber. For a simple homogenous Darcian porous media, the source terms α and β were as follows:

$$\alpha = \frac{1.75\rho(1-\varepsilon)}{\varepsilon^3 D_p}, \beta = \frac{150\mu(1-\varepsilon)^2}{\varepsilon^3 D_p^2}$$

Based on these concepts, 3 sets of Prototype II were developed and tested (Fig. 2 and 3). The size of the box-shaped housing was $30\times 66\times 95$ mm. The membrane surface area was 0.72 m², and its priming volume was 247 ml. The void fraction of these devices was 75 %.

As shown in Fig. 4, the *in vitro* circuit consisted of a blood reservoir in a warm water bath, a roller pump (MERA HAD10; Senko Ikakogyo, Tokyo, Japan), a test device, and a reservoir. A fluid coupled pressure transducer (TP-400T, Nihon Koden Co., Tokyo, Japan) was placed on the inlet and outlet port. These transducers were attached to the monitor (Polygraph System RM-6000, Nihon Koden Co., Tokyo, Japan). A flow probe (Electromagnetic Flow Meter MFV-3200, Nihon Koden Co., Tokyo, Japan) was placed between the inlet port and pump and blood flow was measured using a flow meter (FF-120T, Nihon Koden Co., Tokyo, Japan). Pressure at the inlet and outlet of the device and blood flow rate were monitored continuously. The
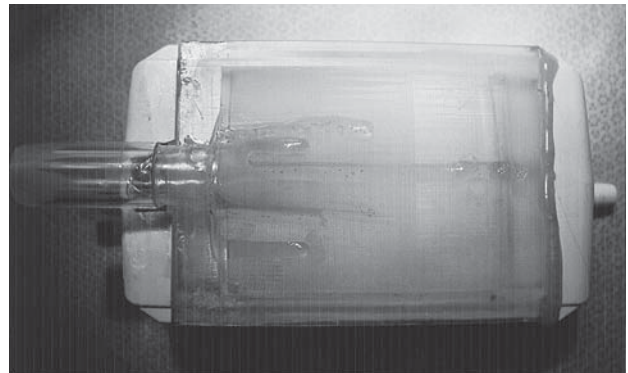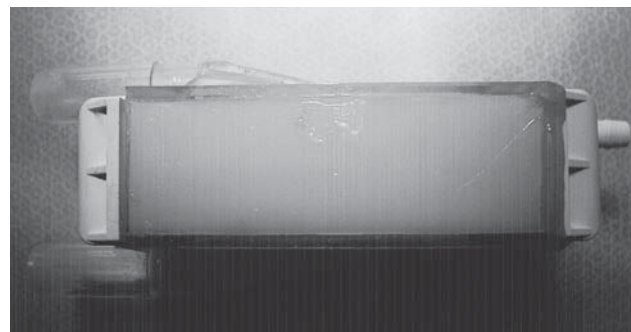

Fig. 2   Prototype II
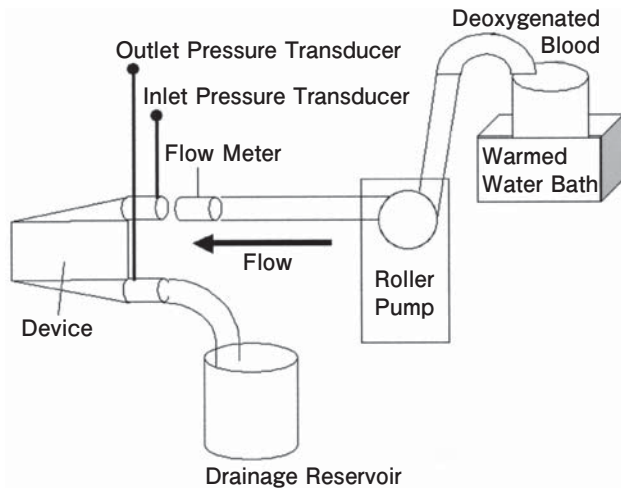

Fig. 3   Lateral view of Prototype II

Fig. 4   Test circuit: Test circuit was consisted of reservoir, roller pump, Prototype II, and drain.

blood flow rate (Q) through the device was given at $\dot{Q}$ = 1, 2, 3 and 5 (L/min). Oxygen was given in the gas path through the device, and the sweep gas flow rate / blood flow rate (V/Q ratio) varied with each flow. V/Q = 1, 2 and 3 in each device. Blood gas analyses were performed using the CIBA-CORNING 280 Blood Gas System (CIBA-CORNING, Tokyo, Japan). Blood samples were taken from both the inlet and outlet ports of the prototype each time the circuit was stopped. Three blood samples were obtained at each data point and then averaged. The anticoagulant ACD-A solution (Terumo CO., Tokyo, Japan) was added to fresh bovine blood to a concentration of 15%. Blood was filtrated using a filter in order to eliminate the hair. The mixed venous blood condition was achieved using a deoxygenator with nitrogen, carbon dioxide (CO_2) and oxygen (O_2) on the other oxygenator. The Prototype II was evaluated according to the suggestions for testing gas exchange devices issued by the Association for Advancement of Medical Instrumentation. The inlet conditions were kept as close as possible to the specified requirements, with the actual conditions being Hb = 12 ± 1 g/dl; SvO_2 = 65.6 ± 5%; PCO_2 = 45 ± 5 mmHg and 37 ± 2 ℃. The viscosity of the blood was adjusted as close as 3.3 cP.

Data analysis. The following formulae were used for calculations of the gas transfer rate ($\dot{V}O_2$ & $\dot{V}CO_2$):

$$\dot{V}O_2 = \dot{Q} \, (C_aO_2 - C_vO_2)$$

$$C_aO_2 = 1.31 \times Hb \times \frac{S_aO_2}{100} + 0.003 \times P_aO_2$$

$$C_vO_2 = 1.31 \times Hb \times \frac{S_vO_2}{100} + 0.003 \times P_vO_2$$

where $\dot{Q}$: blood flow rate; CaO_2: arterial oxygen content; and CvO_2: venous oxygen content; SaO_2: arterial oxygen saturation; SvO_2: venous oxygen saturation,

$$\dot{V}CO_2 = \dot{Q} \, (C_aCO_2 - C_vCO_2)$$

where $\dot{Q}$: blood flow rate; $CaCO_2$: arterial carbon dioxide content; $CvCO_2$: venous carbon dioxide content. $CaCO_2$ & $CvCO_2$ were calculated by Van Slyke & Sendroy's nomogram [5].

Pressure drop (ΔP) was calculated as follows,

$$\Delta P = P_{inlet} - P_{outlet}$$

and resistance (R) was calculated as follows,

$$R = \frac{P_{inlet} - P_{outlet}}{\dot{Q}}$$

where P_{inlet} represents the blood pressure at the inlet port of the device, and P_{outlet} represents the blood pressure at outlet of Prototype II.

Statistical Analyses. Data were expressed as means±SD with a bar graph and error bar. All statistical analyses were performed using univariate analysis of varience within SPSS software (SPSS 12. for Windows, Chicago, IL). R, $\dot{V}O_2$ and $\dot{V}CO_2$ were used as dependent variables; and $\dot{Q}$ and V/Q ratio were used as fixed factors. Pairwise post-hoc comparisons of all $\dot{Q}$ and V/Q ratios were done using Bonferroni. A *p* value less than 0.05 was considered statistically significant.

Results

Fig. 5 shows the volume ratio of the cells which had a flow velocity of 0.007–0.008m/s. The model h15, t80 model had indicated the highest volume ratio at 0.008–0.007m/s. This model was selected as the model to be used for *in vitro* testing, because it had the most constant flow velocity.

Fig. 6 shows the results for the h15, t80 model. In the area of the fiber bundle (the gray area in the middle of the box shape), the cells of fluid velocity were most equally distributed. Resistance across the

device was estimated with CFD and measured in an *in vitro* setting. CFD did not predict the resistance at $\dot{Q} < 1$ L/min. But resistance was well predicted by the CFD model at $\dot{Q} \leq 3$ L/min. In the *in vitro* results, R through the blood path gradually increased with the blood flow rate, but the change was not statistically significant. R at $\dot{Q} = 5$ L/min in Prototype II was 2.7 ± 0.7 mmHg/(L/min) (Fig. 7). VO₂ increased with $\dot{Q}$ significantly ($p < 0.001$), but the V/Q ratio did not have an effect on $\dot{V}O_2$. The value of $\dot{V}O_2$ was at its best, 178 ± 5.3 ml/min at $\dot{Q} = 5$ L/min, V/Q = 3 (Fig. 8). VCO₂ increased both with $\dot{Q}$ and with the V/Q ratio. In terms of $\dot{Q}$, $\dot{V}CO_2$ was

best at $\dot{Q} = 5$ L/min with significance ($p = 0.001$). Also, $\dot{V}CO_2$ was better at V/Q ≥ 2 ($p = 0.017$). $\dot{V}CO_2$ was better at V/Q ≥ 2, but no significant difference was observed in $\dot{V}CO_2$ between the values at V/Q = 2 and at V/Q = 3 (Fig. 9). $\dot{V}CO_2$ was 149 ± 28 ml/min at $\dot{Q} = 5$ L/min and V/Q = 2; $\dot{V}CO_2$ was 133 ± 6.8 ml/min at $\dot{Q} = 5$ L/min and V/Q = 3.

Discussion

As shown in the CFD results (Fig. 5 and 6), the h15, t80 model had the most constant velocity distribution in the fiber bundle area, and it was selected as the basis for developing Prototype II. Equal distribution of velocity is beneficial not only for the gas exchange capacity, but also for the avoidance of stagnation. Currently we do not have thrombus data for this Prototype II, but in the future, this device should be tested in a long-term experiment to confirm the thrombus formation. Resistance through the artificial lung was estimated in CFD, and the result was then compared with the result obtained in an *in vitro* experiment. CFD results corresponded to *in vitro* results at high blood flow rates, $\dot{Q} \geq 3$ L/min (Fig. 7). However, the results were different at low blood flow rates, $\dot{Q} < 1$ L/min. Ergun's law was employed to calculate the result, so the accuracy of the result is known to be low if the Raynord's number (Re) is low, *i.e.*, Re < 1. The other possibility is that the permeability was assumed to be equal in every X, Y, and Z axis. In fact, the permeability can be different because the fiber arrangement is not the same in every axis. In an *in vitro* study, the resistance through the blood path of Prototype II was 2.7 ± 0.7
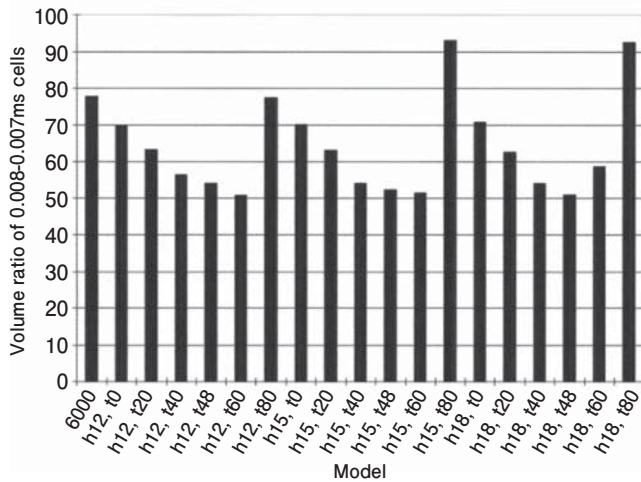
Fig. 5 Volume ratio of cells which had the flow velocity of 0.007-0.008m/s. h = 80, t = 15 model showed the most equal distribution of the flow velocity in fiber bundle area.
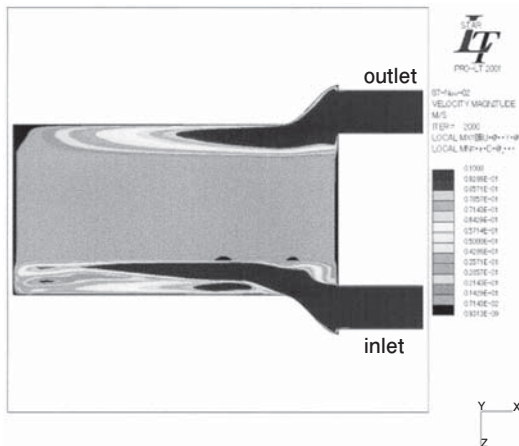
Fig. 6 CFD model results: condensed gray indicated the highest flow velocity area, and black showed the lowest flow velocity area in the legend column. The flow velocity was high at both of inlet and outlet and low in the fiber bundle area.
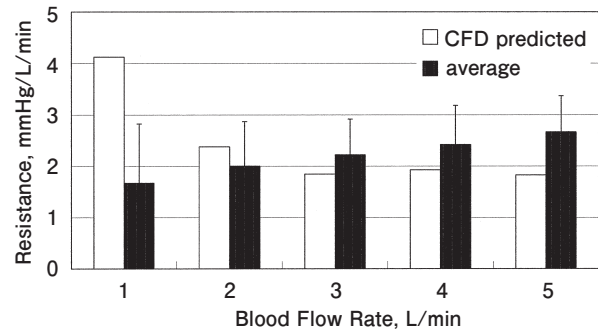
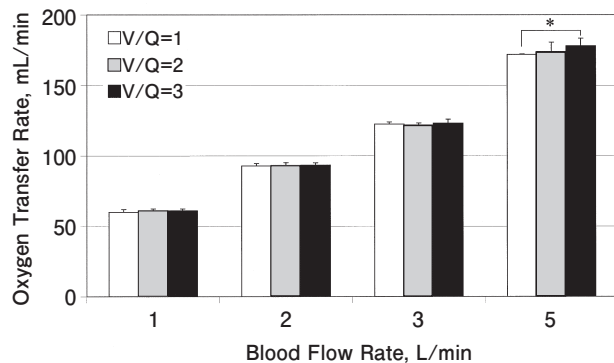**Fig. 7** Resistance predicted by CFD and *in vitro* results in Prototype II

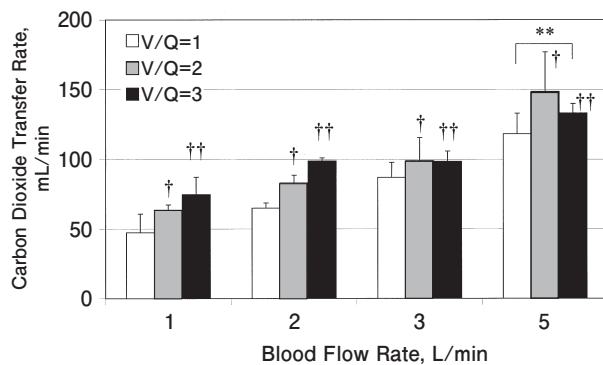**Fig. 8**   Oxygen transfer rate in Prototype II: *: $p < 0.001$ vs. VO_2 at Q = 1, 2 and 3.

Fig. 9   Carbon dioxide transfer rate in Prototype II: **: $p < 0.001$ vs. VCO_2 at Q = 1, 2 and 3 L/min; †: $p = 0.017$ vs. VCO_2 at V/Q =1; ††: $p = 0.006$ vs. VCO_2 at V/Q =1. No significant difference was observed between VCO_2 at V/Q =2 and VCO_2 at V/Q =3.

mmHg/(L/min) at $\dot{Q}$ = 5 L/min. In a large animal study, pulmonary vascular resistance was reported to be approximately 2.8 mmHg/(L/min) [6]. Prototype II showed a resistance low enough to be attached in the pulmonary circulation of large animals, and the gas exchange capacity will be best with around 5 L/min of cardiac output. Currently, this device is being tested with a roller pump, but the right ventricle is pumping the blood with pulsatile flow. In pulsatile flow, impedance is more important than resistance. If impedance data with this device had been obtained under pulsatile flow, the result might be different than the data taken under the flow generated by a roller pump. The $\dot{V}CO_2$ results had a relatively large standard deviation because every device was hand-made, so the arrangement of hollow fibers may have been different between devices. $\dot{V}O_2$ increased with the blood flow rate up to at $\dot{Q}$ = 3 L/

min, and $\dot{V}CO_2$ increased with V/Q ratio up to at V/Q = 2. Prototype II should be used at $\dot{Q} \geq 3$ L/min with V/Q ≥ 2. In general, a human body with a 60kg weight at rest requires $\dot{V}O_2$ = 200 ml/min, $\dot{V}CO_2$ = 120 ml/min. Although in large animals, Prototype II works best at Q ≥ 5 L/min and V/Q ≥ 2, the gas exchange capacity of Prototype II is not sufficient for a human body weight of 60 kg. The membrane surface area of the device should be larger for clinical use. The size of the artificial lung must be small for the purpose of implantation. If the membrane surface area of the artificial lung were larger than that in Prototype II, the size of the device would have to be bigger and it would not fit in the thoracic cage. A compliance chamber might improve this problem. The compliance chamber can attenuate the impedance of the circuit with an artificial lung [7] and may increase the gas exchange capacity without changing the size of the membrane surface area. In terms of gas exchange capacity, steady flow is better than pulsatile flow [8]. The compliance chamber may change the characteristic of the flow [9]. The best compliance with Prototype II should be determined, and an appropriate compliance chamber for Prototype II might increase the gas exchange performance in the future. Prototype II may be implanted in-parallel in the pulmonary circulation. Unlike the oxygenator with a pump, an artificial lung without a pump is set in very low pressure system as pulmonary circulation. In this study, the gas inlet and outlet pressure of Prototype II were not monitored, but Prototype II should be implanted in the pulmonary circulation with the gas inlet and outlet pressure monitored in order to avoid the severe complication of gas being sucked into the blood through the device. The gas exchange capacity deteriorates due to plasma leakage across the fiber wall over long-term use. Accumulated water on the inside of the fiber wall will deteriorate the gas exchange. The most suitable fiber should be determined to avoid these issues so that a more appropriate device can be fabricated for clinical use in the future.

In conclusion, Prototype II can be implanted without a pump in large animals which have a cardiac output around 5 L/min. We believe that Prototype II is an important step on the way to developing an artificial lung without a pump.

References

1. Gartner MJ, Wilhelm CR, Gage KL, Fabrizio MC and Wagner WR: Modeling flow effects on thrombotic deposition in a membrane oxygenator. Artif Organs (2000) 24: 29–36.

2. Gage KL, Gartner MJ, Burgreen GW and Wanger WR: Predicting membrane oxygenator pressure drop using computational fluid dynamics. Artif Organs (2002) 26: 600–607.

3. Kinoshita T, Ichiba S, Aoe M, Shimizu N, Taga I, Funakubo A, Fukui Y and Sakai K: Development of a prototype of implantable artificial lung. ASAIO J (2001) 47: 104.

4. Funakubo A, Taga I, McGillicuddy JB, Fukui Y, Hischl RB and Bartlett RH: Flow vectorial analysis in an artificial implantable lung. ASAIO J (2003) 49: 383–387.

5. Van Slyke, D.D. and Sendroy J: Studies of gas and electrode equilibria in blood. XV. Line charts for graphic calculations by the Henderson-Hasselbalch equation, and for calculating plasma carbon dioxide content from whole blood content. J Biol Chem (1928) 79: 781–798.

6. Haft JW, Montoya P, Alnajjar O, Posner SR, Bull JL, Iannettoni MD, Bartlett RH and Hirschl RB. An artificial lung reduces pulmonary impedance and improves right ventricular efficiency in pulmonary hypertension. J Thorac Cardiovasc Surg (2001) 122: 1094–1100.

7. Lick SD, Zwischenberger JB, Wang D, Deyo DJ, Alpard SK and Chambers SD: Improved right heart function with a compliant inflow artificial lung in series with the pulmonary circulation. Ann Thorac Surg (2001) 72: 899–904.

8. Mockros LF and Leonard RJ: Compact cross-flow tubular oxygenators. Trans ASAIO (1985) 31: 628–632.

9. Boschetti F, Perlman CE, Cook KE and Mockros LF: Hemodynamic effects of attachment modes and device design of a thoracic artificial lung. ASAIO J (2000) 46: 42–48.